Letter

# Excitation spectrum of spin-1 Kitaev spin liquids

Yu-Hsueh Chen [1], Jozef Genzor [1], Yong Baek Kim [2] and Ying-Jer Kao [1,3,*]

[1] *Department of Physics and Center for Theoretical Physics, National Taiwan University, Taipei 10607, Taiwan*
[2] *Department of Physics, University of Toronto, Toronto, Ontario, Canada M5S 1A7*
[3] *Physics Division, National Center for Theoretical Science, National Taiwan University, Taipei 10607, Taiwan*

(Received 23 July 2021; revised 14 January 2022; accepted 24 January 2022; published 7 February 2022)

We study the excitation spectrum of the spin-1 Kitaev model using the symmetric tensor network. By evaluating the virtual order parameters defined on the virtual Hilbert space in the tensor network formalism, we confirm the ground state is in a $\mathbb{Z}_2$ spin-liquid phase. Using the correspondence between the transfer matrix spectrum and low-lying excitations, we find that contrary to the dispersive Majorana excitation in the spin-1/2 case, the isotropic spin-1 Kitaev model has a dispersive bosonic charge excitation. The bottom of the gapped single-particle charge excitations is found at $\mathbf{K}, \mathbf{K}' = (\pm 2\pi/3, \mp 2\pi/3)$, with a corresponding correlation length of $\xi \approx 6.7$ unit cells. The lower edge of the two-particle continuum, which is closely related to the dynamical structure factor measured in inelastic neutron scattering experiments, is obtained by extracting the excitations in the vacuum superselection sector in the anyon theory language.

DOI: 10.1103/PhysRevB.105.L060403

Quantum spin liquids (QSLs) are phases of matter characterized by the existence of long-range entanglement in the ground states and fractionalized excitations [1–3]. The exactly solvable model introduced by Kitaev [4] opens up a new avenue to search for QSL materials in nature that realize Kitaev-like interactions [5–11]. On the other hand, a higher-spin Kitaev model has also been theoretically studied, as the frustrated Ising-like interactions may provide an alternative route to access QSLs [12–14]. Recently, a microscopic mechanism to realize a $S = 1$ Kitaev model and candidate materials have been proposed [15], raising the importance of the study of higher-spin Kitaev physics. Different from its spin-1/2 counterpart, the higher-spin Kitaev model cannot be exactly solved by mapping the spins to Majorana fermions, and numerical studies have been carried out to identify the nature of the ground states for the $S = 1$ Kitaev model [16–21]. While several studies suggest that the isotropic spin-1 Kiatev model exhibits spin liquids with a $\mathbb{Z}_2$ gauge structure, quantitative features about the fractionalized excitations, i.e., the excitation spectrum, are still missing.

The excitation spectrum is deeply connected to the experiments. If the system harbors fractionalized excitations, the dynamical spin structure factor measured in inelastic neutron scattering (INS) should exhibit a broad continuum arising from multiparticle excitations [22]. In the two-dimensional (2D) system, gapped excitations of the QSLs are called anyons, and different types of anyons are distinguished by different superselection sectors [4,23]. To be specific, two particles are in the same sector if there exists a local operator which can transform from one to another. Take the spin-1/2 Kitaev model as an example, where the quasiparticles are $\mathbb{Z}_2$ vortices and fermions [4]. In the anisotropic limit, the system lies in a $\mathbb{Z}_2$ QSL phase with four superselection sectors: vacuum ($I$), charge ($e$), flux ($m$), and fermion ($\epsilon$). In particular, while charge and flux anyons both correspond to the $\mathbb{Z}_2$ vortices, they belong to different sectors since there exists no local operator to transform from one to another. Along this line, one can also deduce that all the even-particle charge, flux, and fermion excitations belong to the same vacuum sector due to the fusion rules $e \times e = m \times m = \epsilon \times \epsilon = I$.

In this Letter, we study the excitation spectrum for the isotropic spin-1 Kitaev model, exploiting the correspondence between the transfer matrix (TM) spectrum and low-energy excitations developed in the tensor network (TN) formalism. We construct a $\mathbb{Z}_2$-invariant projected entangled pair state (PEPS) [24,25] to represent the spin-1 Kitaev model's ground state by applying a loop gas (LG) projector [20,26] on the state generated by imaginary time evolution (ITE) [27]. We identify the nature of $\mathbb{Z}_2$ QSL of the spin-1 Kitaev model by evaluating the virtual order parameters naturally defined in $\mathbb{Z}_2$-invariant PEPS [28]. Due to the fundamental distinction between the integer and half-integer LG projectors [21], we find that in contrast to the dispersive Majorana excitation in $S = 1/2$, the spin-1 Kitaev model possesses a dispersive charge excitation. Furthermore, only the vacuum and charge-anyon sectors are dispersive in the TM spectrum, which shows the existence of the charge excitations with a small gap at the $\mathbf{\Gamma}$, $\mathbf{K}$, and $\mathbf{K}'$ points in the Brillouin zone.

The honeycomb Kitaev model is given by

$$H = -J_x \sum_{\langle i,j\rangle_x} S_i^x S_j^x - J_y \sum_{\langle i,j\rangle_y} S_i^y S_j^y - J_z \sum_{\langle i,j\rangle_z} S_i^z S_j^z, \qquad (1)$$

where $\langle i, j\rangle_\gamma$ represents the nearest-neighboring sites connecting through $\gamma$ links where $\gamma = x, y, z$ [Fig. 1(a)]. There exists a flux operator $W_p = (-1)^{2S} U_1^z U_2^x U_3^y U_4^z U_5^x U_6^y$ which

*yjkao@phys.ntu.edu.tw

 

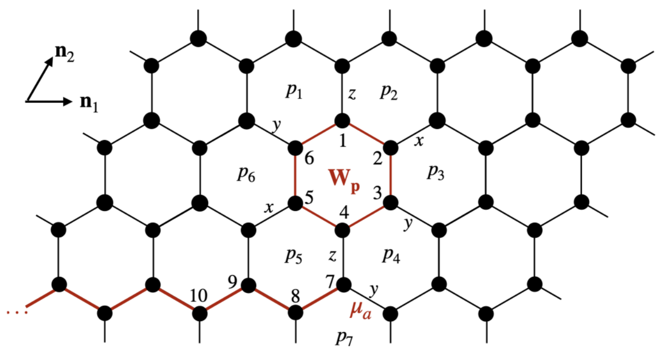


FIG. 1. Honeycomb lattice with the flux operator $W_p$ defined on the plaquette $p$ and the half-infinite string operator $\mu_a$ defined on the link $a = (7, y)$.

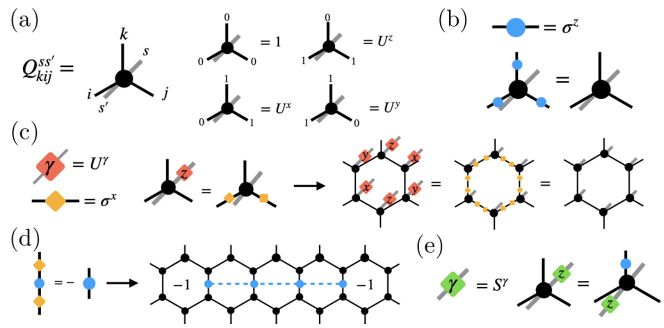

FIG. 2. (a) Definition of the LG tensor $Q^{ss'}_{kij}$. (b) The LG tensor is invariant under the global $\sigma^z$ action on the virtual Hilbert space. (c) The schematic representation of $U^z Q_{kij} = \sum_{i'j'} \sigma^x_{ii'}\sigma^x_{jj'} Q_{ki'j'}$ and the action of the flux operator $W_p$ to the LG operator. (d) A pair of $\mathbb{Z}_2$ vortices can be created by a $\sigma^z$ string on the virtual bonds. (e) The schematic representation of $S^z Q_{kij} = \sum_{k'} \sigma^z_{kk'} Q_{k'ij} S^z$.

commutes with the Hamiltonian, where $U^\gamma = e^{i\pi S^\gamma}$. The Hilbert space is thus divided into sectors according to the eigenvalues of the flux operator $w_p = \pm 1$. In the isotropic case $J_x = J_y = J_z = 1$, the ground state lives in the vortex-free sector $w_p = +1, \forall p$ [12]. Therefore, the states with $w_p = -1$ for a given plaquette $p$ can be understood as a $\mathbb{Z}_2$ vortex quasiparticle. On the other hand, one can define a half-infinite string operator $\mu_a = \prod_{n=i}^{\infty} (i)^{2S} U_n^{\gamma_n}$ labeled by $a = (i, \gamma)$ for a given link $\gamma$ attached to site $i$. Here, $(i, i+1, \ldots)$ are sites traversed by the string and $(\gamma_i, \gamma_{i+1}, \ldots)$ are links normal to the string. For instance, the string operator $\mu_a$ with $a = (7, y)$ in Fig. 1 is $\prod_{n=7}^{\infty} (i)^{2S} U_n^z$. In the vortex-free sector, the path of the string is irrelevant since one can deform the path by applying $W_p$ without changing the wave function. Therefore, one can regard the starting point of the string operator as a topologically nontrivial excitation. This operator is the same disorder operator defined in Ref. [12], where by attaching specific operators to the starting point of $\mu_a$, one can construct a set of operators acting as Majorana fermions and hard-core bosons for the half-integer and integer spin, respectively.

The qualitative difference between the integer and half-integer Kitaev models can be understood through the identities

$$U^\alpha U^\beta = \begin{cases} \delta^{\alpha\beta}\mathbb{I} + |\epsilon^{\alpha\beta\gamma}| U^\gamma, & S = 0, 1, \ldots, \\ -\delta^{\alpha\beta}\mathbb{I} + \epsilon^{\alpha\beta\gamma} U^\gamma, & S = 1/2, 3/2, \ldots, \end{cases} \quad (2)$$

where $\epsilon^{\alpha\beta\gamma}$ is the Levi-Civita symbol. Consider moving a $\mathbb{Z}_2$ vortex around the central plaquette $p$ with $w_p = -1$ following the path $p_1 \to p_2 \to \cdots \to p_6$ in Fig. 1. For the half-integer spin, the action of moving the vortex from $p_1$ to $p_2$ can be done by $U_1^z$ since $\{W_{p_1}, U_1^z\} = \{W_{p_2}, U_1^z\} = 0$ due to the relation $\{U_1^y, U_1^z\} = \{U_1^x, U_1^z\} = 0$. Therefore, the operator moving a $\mathbb{Z}_2$ vortex around the central plaquette is exactly the flux operator $W_p = U_1^z U_2^x U_3^y U_4^z U_5^x U_6^y$, leading to the $\pi$ phase shift as $w_p = -1$. This nontrivial mutual statistics makes the half-integer spin Kitaev models become the toric code Hamiltonian in the anisotropic limit ($J_z \gg J_x, J_y$), where the charge and flux anyons both correspond to the $\mathbb{Z}_2$ vortices but live in alternating rows of plaquettes [4,13]. The half-infinite string operator $\mu_a$ in Fig. 1 then corresponds to the creation of two vortices, i.e., the charge-flux composite (gauge fermion), at $p_4$ and $p_7$. On the other hand, for the integer spin, $U^\gamma$ cannot move the vortex since $[U^\alpha, U^\beta] = 0$ for $\alpha \neq \beta$. While one can move the vortex around the central plaquette by applying another loop operator $S_1^z S_2^x S_3^y S_4^z S_5^x S_6^y$ since $\{U^\alpha, S^\beta\} = 0$ ($\alpha \neq \beta$), this operator does not commute with the Hamiltonian and thus cannot give back to the original state. Whether the $\mathbb{Z}_2$ vortices in alternating rows belong to different superselection sectors and their relation with $\mu_a$ is unclear.

The LG projector [20,26] provides a natural connection between the $\mathbb{Z}_2$ vortex and the half-infinite string operator $\mu_a$. The integer spin LG projector is defined as $Q_{\mathrm{LG}} = \mathrm{tTr} \prod_\alpha Q^{ss'}_{k_\alpha i_\alpha j_\alpha} |s\rangle\langle s'|$ with the nonzero elements of the LG tensor as [Fig. 2(a)] [21]

$$Q_{000} = \mathbb{I}, \quad Q_{011} = U^z, \quad Q_{101} = U^x, \quad Q_{110} = U^y. \quad (3)$$

By construction, the LG tensor is invariant under the global $\mathbb{Z}_2$ action on the virtual Hilbert space, $Q(u_g \otimes u_g \otimes u_g) = Q$ with $g \in \{I, Z\}$ and $u_I = \mathbb{I}_2$, $u_Z = \sigma^z$ [Fig. 2(b)]. A tensor $T$ contracted with the LG tensor $\tilde{T}^s_{kk_0,ii_0,jj_0} = \sum_{s'} Q^{ss'}_{k,i,j} T^{s'}_{k_0,i_0,j_0}$ acquires the virtual $\mathbb{Z}_2$ symmetry with $u_I = \mathbb{I}_2 \otimes_\alpha \mathbb{I}_{D_0}$, $u_Z = \sigma^z \otimes \mathbb{I}_{D_0}$, where $D_0$ is the bond dimension of the original tensor $T$. The wave functions formed by contracting the virtual bonds of $\tilde{T}$ is then called a $\mathbb{Z}_2$-invariant PEPS [24,25]. On the other hand, the LG tensor satisfies the *physical-virtual relation* $U^z Q_{kij} = \sum_{i'j'} \sigma^x_{ii'}\sigma^x_{jj'} Q_{ki'j'}$ (and similar relations for $U^x$, $U^y$), making $Q_{\mathrm{LG}}$ a projector to the vortex-free space: $W_p Q_{\mathrm{LG}} = Q_{\mathrm{LG}} W_p = Q_{\mathrm{LG}}$ [Fig. 2(c)]. Remarkably, this physical-virtual relation transforms the half-infinite string operator $\mu_a$ in Fig. 1 to the local virtual $\sigma^x$ action on the $y$ link shared by $p_4$ and $p_7$. In addition, using $\sigma^x\sigma^z\sigma^x = -\sigma^z$, one can show that a pair of $\mathbb{Z}_2$ vortices can be created by a $\sigma^z$ string on the virtual bonds [Fig. 2(d)], meaning that a single $\sigma^z$ on the virtual bond can be used to move the $\mathbb{Z}_2$ vortex. One can then naturally interpret all the $\mathbb{Z}_2$ vortices as flux anyons and the end point of $\mu_a$ as a charge anyon since moving the vortex around $a = (7, y)$ through $p_5 \to p_4 \to p_7$ acquires a nontrivial $\pi$ phase due to the presence of $\sigma^x$ action. In fact, the corresponding virtual actions of $\mu_a$ and the $\mathbb{Z}_2$ vortex are exactly the creation of the charge and flux anyon in the framework of $\mathbb{Z}_2$-invariant PEPS [29] (see the Supplemental Material [30] for details).

In the following, we focus on the isotropic Kitaev model ($J_z = J_x = J_y = 1$). Different from Ref. [20] where the LG projected state is used as an initial trial wave function for the ITE, we apply the LG projector at the end to obtain a $\mathbb{Z}_2$-invariant ground state. In other words, we first perform the ITE and then apply the LG projector to the resulting state, i.e., $|\psi\rangle = \lim_{\tau\to\infty} Q_{\rm LG} e^{-\tau H}|\psi_0\rangle$. Here, the initial product state $|\psi_0\rangle = \otimes_\alpha |(111)\rangle_\alpha$, where $|(111)\rangle$ is the magnetized state along the (1,1,1) direction. This ensures that the PEPS with a fixed bond dimension $D$ is vortex free and satisfies all the nice properties inherited from the LG projector. Another interesting property of this construction is that $S^z Q_{kij} = \sum_{k'} \sigma^z_{kk'} Q_{k'ij} S^z$ (and similar relations for $S^x, S^y$) [Fig. 2(e)], which indicates that $S^z$ will not only move the vortex but change the ITE wave function to $S^z e^{-\tau H}|\psi_0\rangle$, making the previous argument that the loop operator $S^z_1 S^x_2 S^y_3 S^z_4 S^x_5 S^y_6$ will change the ground state more obvious. It is the LG projector that allows us to manipulate the vortex on the virtual bonds using $\sigma^z$ without spoiling the wave function. In addition, our construction allows for a lower computational cost than that of the gauge-symmetry-preserved update [31,32], as only half of the bond dimension is needed during the ITE process.

While the LG projector forms a natural framework to describe $\mathbb{Z}_2$ QSLs, the topological property of the projected wave function also depends on the initial trial state. For instance, it is possible to have $|\psi\rangle = \mu_a|\psi\rangle$ for some state $|\psi\rangle = Q_{\rm LG}|\psi_{\rm trial}\rangle$. In this case, the half-infinite string operator $\mu_a$ which should create a charge anyon actually does nothing to the ground state, and thus the charge is condensed. Similarly, if $\langle\psi_{\rm ex}|\psi_{\rm ex}\rangle = 0$, the system is in a charge confined phase [28,29,33]. Therefore, to nail down the nature of the isotropic spin-1 Kitaev model, one should make sure $\mu_a$ actually creates a proper excitation. In other words, we should consider the overlap of the wave functions $\langle\psi_{\rm ex}|\psi_{\rm ex}\rangle$ and $\langle\psi_{\rm ex}|\psi\rangle$ where $|\psi_{\rm ex}\rangle = \mu_a|\psi\rangle$.

As stated previously, the effect of $\mu_a$ is equivalent to applying a local $\sigma^x$ on the virtual bond using the physical-virtual relation in Fig. 2(c); therefore, the overlap of the charge excited state can be evaluated easily in the virtual Hilbert space. To calculate those quantities, we consider the transfer matrix (TM) $\mathbb{T} \equiv \lim_{L_x\to\infty} {\rm tTr}(\mathbb{E}^1\mathbb{E}^2\cdots\mathbb{E}^{L_x})$ with $\mathbb{E}$ the double tensor formed by contracting the physical indices of the local tensor $A$ and its adjoint $A^*$. The TM can be regarded as the building block of the norm of the two-dimensional PEPS, $\langle\psi|\psi\rangle = (l|\lim_{L_y\to\infty}\mathbb{T}^{L_y}|r) = (l|[\lim_{L_y\to\infty}|l)\lambda^{L_y}(r|]|r)$, where $|l)$ [$|r)$] is the left (right) dominant eigenvector of $\mathbb{T}$ and $\lambda$ is the corresponding dominant eigenvalue which is normalized to 1. Here, we use $|\cdot)$ to denote a vector defined in the virtual Hilbert space. In our case, $|l)$ and $|r)$ are the same and we denote them as $|\rho)$ in the following. It is then obvious that the overlap of the wave functions $\langle\psi_{\rm ex}|\psi\rangle$ and $\langle\psi_{\rm ex}|\psi\rangle$ corresponds to the *virtual order parameters* $(\rho|\sigma^x\otimes\mathbb{I}|\rho)$ and $(\rho|\sigma^x\otimes\sigma^x|\rho)$. Therefore, the system is in the topologically ordered phase only when $(\rho|\sigma^x\otimes\mathbb{I}|\rho)\neq 0$ and $(\rho|\sigma^x\otimes\mathbb{I}|\rho) = 0$. To evaluate the order parameters in the infinite two-dimensional TN, we employ the variational uniform matrix product state (VUMPS) algorithm [34–36] whose accuracy can be controlled by the bond dimension of MPS $D_{\rm mps}$ [30]. Throughout the calculation, we find that $(\rho|\sigma^x\otimes\sigma^x|\rho) = 1$ and $(\rho|\sigma^x\otimes\mathbb{I}|\rho) = 0$ regardless of the bond dimension (up to $D = 10$), suggesting that the system lies in the $\mathbb{Z}_2$ spin-liquid phase. This method has an advantage over identifying the QSL phase by topological entanglement entropy, which is limited by a small bond dimension and suffers from the finite-size effect [20].

The TM's subdominant eigenvalues encompass signatures of the low-energy excitations [33,37–40]. This is a manifestation of the fact that the information of a local Hamiltonian's excitations is encoded in the ground state, which can be extracted by measuring the ground-state correlations. The prominent example is that the minus logarithm of the largest subleading eigenvalue $-\log|\lambda|$, which corresponds to the inverse of the correlation length $\xi$, can be related to the spectral gap up to an overall energy scale [41]. This argument has been further extended in Ref. [37] to include the momentum dependence. To be specific, for a generally complex eigenvalue $\lambda = e^{-\epsilon+i\phi}$ of the TM, the corresponding physical excitation energy is given as $E\sim\epsilon = -\log|\lambda|$, while the corresponding momentum is related to the phase $k\sim\phi = \arg\lambda$. Therefore, by solving the eigenvalue problem of the *transfer matrix Hamiltonian* $H_{\mathbb{T}} = -\log\mathbb{T}$, one can access the physical Hamiltonian's low-lying excitations. The fixed point $|\rho)$ now corresponds to the ground state of the TM Hamiltonian $H_{\mathbb{T}}$ since the energy $\epsilon = -\log|\lambda| = 0$. Since the TM Hamiltonian is one dimensional, the excitations for this Hamiltonian, which we term TM excitations, can be studied by constructing the excitation ansatz on top of the fixed point [36,42]. Note that if the TM has a zero subleading eigenvalue, i.e., $\lambda = 0$, it implies that elementary excitation is static since the correlation length $\xi = -1/\log|\lambda|$ is zero. In addition, the nondispersive nature of the static excitation can be observed by noting that there is no low-lying momentum as the corresponding momentum $k\sim\phi$ is not well defined.

In the $\mathbb{Z}_2$ topologically ordered phase, the TM excitations can be divided into four types, which correspond to physical excitations belonging to four superselection sectors [33]. The ground-state wave function's norm can be obtained from the TM. However, if there exist locally indistinguishable degenerate ground states, the TM should also contain the overlap of different ground states. For the spin-1 Kitaev model, the ground-state subspace is spanned by the basis $|(\pm)_1(\pm)_2\rangle$ labeled by the eigenvalues $(\pm 1)$ of the global Wilson loop operators $W_1 = \prod_{i\in L_1}^{\infty}(i)^{2S}U^z_n$ and $W_2 = \prod_{i\in L_2}^{\infty}(i)^{2S}U^y_n$ with $L_1$ ($L_2$) the noncontractible path along the $\mathbf{n_1}$ ($\mathbf{n_2}$) direction in Fig. 1. Here, the global Wilson loop operator $W_1$ ($W_2$) can be understood as a process of creating a pair of charge anyons, wrapping them around $L_1$ ($L_2$), and finally annihilating them. To relate the ground-state overlap to the anyonic excitations, we consider the basis of minimally entangled states (MES) defined as $|\psi(I)\rangle = |++\rangle + |-+\rangle$, $|\psi(e)\rangle = |++\rangle - |-+\rangle$, $|\psi(m)\rangle = |+-\rangle + |--\rangle$, and $|\psi(\epsilon)\rangle = |+-\rangle - |--\rangle$ [43]. The TM can then be divided into four sectors corresponding to different MES overlaps: $\mathbb{T}_{\langle I|I\rangle}$, $\mathbb{T}_{\langle I|e\rangle}$, $\mathbb{T}_{\langle I|m\rangle}$, and $\mathbb{T}_{\langle I|\epsilon\rangle}$ [44]. Since applying the Wilson operator characterized by different anyons along $L_1$ to the vacuum state generates a new MES [43], one can relate the TM excitations from $\mathbb{T}_{\langle I|a\rangle}$ with $a = e, m, \epsilon$ to the physical charge, flux, and fermion (charge-flux composite) excitations [33,37]. On the other hand, TM excitations from $\mathbb{T}_{\langle I|I\rangle}$ have no anyonic difference between the ket and bra states; hence they belong to the vacuum, i.e., topologically trivial, excitations. Using this correspondence, one can probe different anyonic excitations

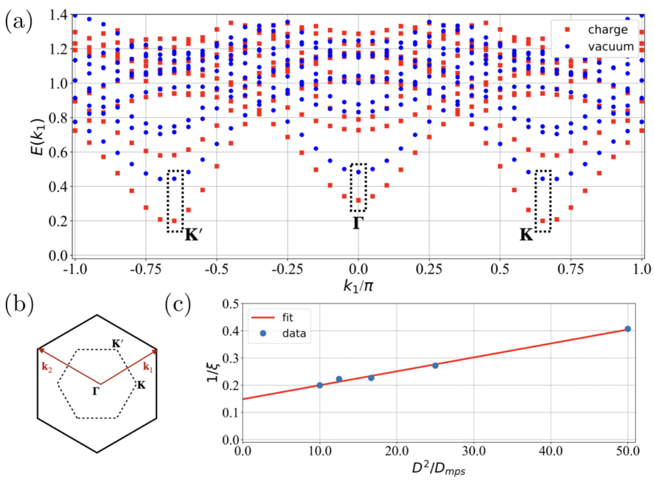


FIG. 3. (a) Transfer matrix spectrum for the PEPS tensor with $(D, D_{\rm mps}) = (10, 10)$. (b) Brillouin zone with labeled positions of the minimum of TM spectrum. (c) The inverse of the correlation length of the $D = 10$ PEPS wave function as a function of $D_{\rm mps}$.

by distinguishing the TM spectrum with appropriate quantum numbers defined on the virtual Hilbert space [30].

Interestingly, for the spin-1 Kitaev model, we find that $\lambda_{\langle I|m\rangle} = \lambda_{\langle I|\epsilon\rangle} = 0$, indicating there are no TM excitations belonging to the $\mathbb{T}_{\langle I|m\rangle}$ and $\mathbb{T}_{\langle I|\epsilon\rangle}$ sectors. This shows that the LG projector for the integer spins only supports dispersive excitations belonging to the vacuum and charge sectors, while the flux- and fermion-sector excitations are static. This is intrinsically different from the half-integer LG projector, where only vacuum and fermion excitations are dispersive [44]. In addition, this is consistent with the argument put forth in Ref. [12] that the integer-spin Kitaev model has bosonic exciations instead of Majorana fermions, indicating that the different sign structures of the integer and half-integer spin LG projectors may faithfully describe the distinct nature of the integer and half-integer spin Kitaev models [21].

Using the correspondence $E_{k_1} \sim -\log|\lambda_{k_1}|$ for a given momentum $k_1$ in the $x$ direction, the TM spectra for PEPS states with bond dimension $D = 10$ are shown in Fig. 3(a). The excitations belonging to charge and vacuum sectors are labeled by red and blue colors, respectively. While the overall energy scale of the minimum of $E_{k_1}$ and exact excitation energies are unknown due to the lack of the knowledge of the Lieb-Robinson velocity [45], the corresponding momentum $k_1$ at the local minimum of $E_{k_1}$ allows us to identify the location of the low-energy dispersion [41]. It then follows that both the charge- and vacuum-sector excitations are clearly identified at $k_1 = 0$, $2\pi/3$, and $-2\pi/3$. We also perform the corner transfer matrix renormalization group (CTMRG) [46–48] to obtain the TM spectrum [30], and the results are consistent. To gain more insights into the two-dimensional system, we consider the momentum in the $y$ direction using $k_2 \sim \arg\lambda_{k_1}$. The locations of three minimum excitations are then identified at $(k_1, k_2) = (0, 0)$, $(2\pi/3, -2\pi/3)$, and $(-2\pi/3, 2\pi/3)$, suggesting that the spin-1 Kitaev model harbors three low-lying charge anyon excitations at the $\mathbf{\Gamma}$, $\mathbf{K}$, and $\mathbf{K}'$ points in the Brillouin zone [Fig. 3(b)]. To nail down the origin of the vacuum-sector excitations, which correspond to all possible even-particle excitations, we note that the global minima lie at $\mathbf{K}$ ($\mathbf{K}'$): $\epsilon_{\rm min} = \epsilon(\mathbf{K}) = \epsilon(\mathbf{K}') < \epsilon(\mathbf{\Gamma})$. The low-lying vacuum-sector excitations at $\mathbf{\Gamma}$, $\mathbf{K}$, and $\mathbf{K}'$ can then be well explained by attributing to the two-particle charge excitations $\epsilon(\mathbf{K}) + \epsilon(\mathbf{K}')$, $\epsilon(\mathbf{K}') + \epsilon(\mathbf{K}')$, and $\epsilon(\mathbf{K}) + \epsilon(\mathbf{K})$, respectively. Therefore, we conclude that the excitations belonging to the vacuum sector describe the minima of the two-particle continuum.

Figure 3(c) shows the the inverse of the correlation length, i.e., the corresponding charge excitation energy at $\mathbf{K}$ ($\mathbf{K}'$), as a function of the accuracy-controlled dimension $D_{\rm mps}$. Extrapolation to $D_{\rm mps} \to \infty$ shows that the system is gapped with a correlation length of $\xi \approx 6.7$ unit cells. Using the excitation gap $E_{24\ \rm site} \approx 3.6 \times 10^{-2}$ from a 24-site exact diagonalization [16] as the upper bound, we estimate the characteristic velocity $\upsilon_{\rm LR} \approx 2.4 \times 10^{-1}$ using the relation $\xi E_{24\ \rm site} = \upsilon_{\rm LR}$ [37,41].

In this Letter, we find that the spin-1 Kitaev model harbors bosonic excitations and locate the single- and two-particle excitations' minima at $\mathbf{\Gamma}$, $\mathbf{K}$, and $\mathbf{K}'$. Note that the dynamical spin structure factor, which allows a direct comparison with the INS experiment, involves not only the two-particle excitation, but also the static gauge flux as the spin-flip operator will necessarily induce a flux anyon pair [49–51]. This makes the connection between the INS experiments with the two-particle excitations less trivial. However, we note that the resonant inelastic x-ray scattering experiments may provide a route to single out the Majorana sector without the influence of flux in the spin-1/2 Kitaev model [52]. It is interesting to further investigate whether a similar scheme can be applied to the spin-1 case to detect the signal from the charge sector only. We also remark that directly computing the dynamical structure factor using the technique developed in Ref. [53] is feasible and worth exploring. On the other hand, the construction of the $\mathbb{Z}_2$-invariant PEPS using the LG projector is an efficient method to separate different anyonic excitations and can be easily generalized to the anisotropic Kitaev model. By tracing the evolution of the excitation spectra, one should be able to understand whether the QSL feature in the isotropic Kitaev model persists when the system is driven away from the isotropic point.

## ACKNOWLEDGMENTS

This work is partially supported by the Ministry of Science and Technology (MOST) of Taiwan under Grants No. 107-2112-M-002-016-MY3 and No. 108-2112-M-002-020-MY3 (Y.H.C., J.Z., Y.J.K.). Y.B.K. is supported by the NSERC of Canada and the Center for Quantum Materials at the University of Toronto.

[1] L. Savary and L. Balents, Quantum spin liquids: A review, Rep. Prog. Phys. 80, 016502 (2016).

[2] Y. Zhou, K. Kanoda, and T.-K. Ng, Quantum spin liquid states, Rev. Mod. Phys. 89, 025003 (2017).

[3] C. Broholm, R. J. Cava, S. A. Kivelson, D. G. Nocera, M. R. Norman, and T. Senthil, Quantum spin liquids, Science **367**, 6475 (2020).

[4] A. Kitaev, Anyons in an exactly solved model and beyond, Ann. Phys. **321**, 2 (2006).

[5] G. Jackeli and G. Khaliullin, Mott Insulators in the Strong Spin-Orbit Coupling Limit: From Heisenberg to a Quantum Compass and Kitaev Models, Phys. Rev. Lett. **102**, 017205 (2009).

[6] Y. Singh, S. Manni, J. Reuther, T. Berlijn, R. Thomale, W. Ku, S. Trebst, and P. Gegenwart, Relevance of the Heisenberg-Kitaev Model for the Honeycomb Lattice Iridates $A_2IrO_3$, Phys. Rev. Lett. **108**, 127203 (2012).

[7] W. Witczak-Krempa, G. Chen, Y. B. Kim, and L. Balents, Correlated quantum phenomena in the strong spin-orbit regime, Annu. Rev. Condens. Matter Phys. **5**, 57 (2014).

[8] J. G. Rau, E. K.-H. Lee, and H.-Y. Kee, Spin-orbit physics giving rise to novel phases in correlated systems: Iridates and related materials, Annu. Rev. Condens. Matter Phys. **7**, 195 (2016).

[9] S. M. Winter, A. A. Tsirlin, M. Daghofer, J. van den Brink, Y. Singh, P. Gegenwart, and R. Valentí, Models and materials for generalized Kitaev magnetism, J. Phys.: Condens. Matter **29**, 493002 (2017).

[10] K. W. Plumb, J. P. Clancy, L. J. Sandilands, V. V. Shankar, Y. F. Hu, K. S. Burch, H.-Y. Kee, and Y.-J. Kim, $\alpha$-$RuCl_3$: A spin-orbit assisted Mott insulator on a honeycomb lattice, Phys. Rev. B **90**, 041112(R) (2014).

[11] Y. Kasahara, T. Ohnishi, Y. Mizukami, O. Tanaka, S. Ma, K. Sugii, N. Kurita, H. Tanaka, J. Nasu, Y. Motome *et al.*, Majorana quantization and half-integer thermal quantum Hall effect in a Kitaev spin liquid, Nature (London) **559**, 227 (2018).

[12] G. Baskaran, D. Sen, and R. Shankar, Spin-$S$ Kitaev model: Classical ground states, order from disorder, and exact correlation functions, Phys. Rev. B **78**, 115116 (2008).

[13] T. Minakawa, J. Nasu, and A. Koga, Quantum and classical behavior of spin-$S$ Kitaev models in the anisotropic limit, Phys. Rev. B **99**, 104408 (2019).

[14] J. Oitmaa, A. Koga, and R. R. P. Singh, Incipient and well-developed entropy plateaus in spin-$S$ Kitaev models, Phys. Rev. B **98**, 214404 (2018).

[15] P. P. Stavropoulos, D. Pereira, and H.-Y. Kee, Microscopic Mechanism for a Higher-Spin Kitaev Model, Phys. Rev. Lett. **123**, 037203 (2019).

[16] A. Koga, H. Tomishige, and J. Nasu, Ground-state and thermodynamic properties of an $S = 1$ Kitaev model, J. Phys. Soc. Jpn. **87**, 063703 (2018).

[17] X.-Y. Dong and D. N. Sheng, Spin-1 Kitaev-Heisenberg model on a honeycomb lattice, Phys. Rev. B **102**, 121102(R) (2020).

[18] Z. Zhu, Z.-Y. Weng, and D. N. Sheng, Magnetic field induced spin liquids in $S = 1$ Kitaev honeycomb model, Phys. Rev. Research **2**, 022047(R) (2020).

[19] I. Khait, P. P. Stavropoulos, H.-Y. Kee, and Y. B. Kim, Characterizing spin-one Kitaev quantum spin liquids, Phys. Rev. Research **3**, 013160 (2021).

[20] H.-Y. Lee, N. Kawashima, and Y. B. Kim, Tensor network wave function of $S = 1$ Kitaev spin liquids, Phys. Rev. Research **2**, 033318 (2020).

[21] H.-Y. Lee, T. Suzuki, Y. B. Kim, and N. Kawashima, Anisotropy as a diagnostic test for distinct tensor-network wave functions of integer- and half-integer-spin Kitaev quantum spin liquids, Phys. Rev. B **104**, 024417 (2021).

[22] R. Coldea, D. A. Tennant, A. M. Tsvelik, and Z. Tylczynski, Experimental Realization of a 2D Fractional Quantum Spin Liquid, Phys. Rev. Lett. **86**, 1335 (2001).

[23] A. Kitaev and C. Laumann, Topological phases and quantum computation, arXiv:0904.2771.

[24] N. Schuch, I. Cirac, and D. Pérez-García, PEPS as ground states: Degeneracy and topology, Ann. Phys. **325**, 2153 (2010).

[25] N. Schuch, D. Poilblanc, J. I. Cirac, and D. Pérez-García, Resonating valence bond states in the PEPS formalism, Phys. Rev. B **86**, 115108 (2012).

[26] H.-Y. Lee, R. Kaneko, T. Okubo, and N. Kawashima, Gapless Kitaev Spin Liquid to Classical String Gas through Tensor Networks, Phys. Rev. Lett. **123**, 087203 (2019).

[27] H. C. Jiang, Z. Y. Weng, and T. Xiang, Accurate Determination of Tensor Network State of Quantum Lattice Models in Two Dimensions, Phys. Rev. Lett. **101**, 090603 (2008).

[28] M. Iqbal and N. Schuch, Entanglement Order Parameters and Critical Behavior for Topological Phase Transitions and Beyond, Phys. Rev. X **11**, 041014 (2021).

[29] K. Duivenvoorden, M. Iqbal, J. Haegeman, F. Verstraete, and N. Schuch, Entanglement phases as holographic duals of anyon condensates, Phys. Rev. B **95**, 235119 (2017).

[30] See Supplemental Material at http://link.aps.org/supplemental/10.1103/PhysRevB.105.L060403 for details about $\mathbb{Z}_2$-invariant PEPS and how it is applied to the spin-1 Kitaev model, methods about using VUMPS to calculate VOPs and TM excitations, and the TM spectrum calculated using CTMRG.

[31] H. He, H. Moradi, and X.-G. Wen, Modular matrices as topological order parameter by a gauge-symmetry-preserved tensor renormalization approach, Phys. Rev. B **90**, 205114 (2014).

[32] J.-W. Mei, J.-Y. Chen, H. He, and X.-G. Wen, Gapped spin liquid with $\mathbb{Z}_2$ topological order for the Kagome Heisenberg model, Phys. Rev. B **95**, 235107 (2017).

[33] J. Haegeman, V. Zauner, N. Schuch, and F. Verstraete, Shadows of anyons and the entanglement structure of topological phases, Nat. Commun. **6**, 8284 (2015).

[34] V. Zauner-Stauber, L. Vanderstraeten, M. T. Fishman, F. Verstraete, and J. Haegeman, Variational optimization algorithms for uniform matrix product states, Phys. Rev. B **97**, 045145 (2018).

[35] M. T. Fishman, L. Vanderstraeten, V. Zauner-Stauber, J. Haegeman, and F. Verstraete, Faster methods for contracting infinite two-dimensional tensor networks, Phys. Rev. B **98**, 235148 (2018).

[36] L. Vanderstraeten, J. Haegeman, and F. Verstraete, Tangent-space methods for uniform matrix product states, SciPost Phys. Lect. Notes **7**, 51 (2019).

[37] V. Zauner, D. Draxler, L. Vanderstraeten, M. Degroote, J. Haegeman, M. M. Rams, V. Stojevic, N. Schuch, and F. Verstraete, Transfer matrices and excitations with matrix product states, New J. Phys. **17**, 053002 (2015).

[38] Y.-C. He, M. P. Zaletel, M. Oshikawa, and F. Pollmann, Signatures of Dirac Cones in a DMRG Study of the Kagome Heisenberg Model, Phys. Rev. X **7**, 031020 (2017).

[39] M. Gohlke, G. Wachtel, Y. Yamaji, F. Pollmann, and Y. B. Kim, Quantum spin liquid signatures in Kitaev-like frustrated magnets, Phys. Rev. B **97**, 075126 (2018).

[40] S. Hu, W. Zhu, S. Eggert, and Y.-C. He, Dirac Spin Liquid on the Spin-1/2 Triangular Heisenberg Antiferromagnet, Phys. Rev. Lett. **123**, 207203 (2019).

[41] M. B. Hastings, Locality in Quantum and Markov Dynamics on Lattices and Networks, Phys. Rev. Lett. **93**, 140402 (2004).

[42] J. Haegeman, B. Pirvu, D. J. Weir, J. I. Cirac, T. J. Osborne, H. Verschelde, and F. Verstraete, Variational matrix product ansatz for dispersion relations, Phys. Rev. B **85**, 100408(R) (2012).

[43] Y. Zhang, T. Grover, A. Turner, M. Oshikawa, and A. Vishwanath, Quasiparticle statistics and braiding from ground-state entanglement, Phys. Rev. B **85**, 235151 (2012).

[44] Y.-H. Chen, C.-Y. Huang, and Y.-J. Kao, Detecting transition between Abelian and non-Abelian topological orders through symmetric tensor networks, Phys. Rev. B **104**, 045131 (2021).

[45] E. H. Lieb and D. W. Robinson, The finite group velocity of quantum spin systems, Commun. Math. Phys. **28**, 251 (1972).

[46] T. Nishino and K. Okunishi, Corner transfer matrix renormalization group method, J. Phys. Soc. Jpn. **65**, 891 (1996).

[47] R. Orús and G. Vidal, Simulation of two-dimensional quantum systems on an infinite lattice revisited: Corner transfer matrix for tensor contraction, Phys. Rev. B **80**, 094403 (2009).

[48] P. Corboz, J. Jordan, and G. Vidal, Simulation of fermionic lattice models in two dimensions with projected entangled-pair states: Next-nearest neighbor Hamiltonians, Phys. Rev. B **82**, 245119 (2010).

[49] G. Baskaran, S. Mandal, and R. Shankar, Exact Results for Spin Dynamics and Fractionalization in the Kitaev Model, Phys. Rev. Lett. **98**, 247201 (2007).

[50] J. Knolle, D. L. Kovrizhin, J. T. Chalker, and R. Moessner, Dynamics of a Two-Dimensional Quantum Spin Liquid: Signatures of Emergent Majorana Fermions and Fluxes, Phys. Rev. Lett. **112**, 207203 (2014).

[51] J. Knolle, D. L. Kovrizhin, J. T. Chalker, and R. Moessner, Dynamics of fractionalization in quantum spin liquids, Phys. Rev. B **92**, 115127 (2015).

[52] G. B. Halász, N. B. Perkins, and J. van den Brink, Resonant Inelastic X-ray Scattering Response of the Kitaev Honeycomb Model, Phys. Rev. Lett. **117**, 127203 (2016).

[53] M. Gohlke, R. Verresen, R. Moessner, and F. Pollmann, Dynamics of the Kitaev-Heisenberg Model, Phys. Rev. Lett. **119**, 157203 (2017).